

## CALCULATION OF THE TIME-TO-FLOOD OF A BOX-SHAPED BARGE BY USING CFD

C. Strasser<sup>1</sup>, A. Jasionowski<sup>2</sup> and D. Vassalos<sup>2</sup>

### ABSTRACT

This paper addresses the assessment of the damage survivability of a fictitious model of a box-shaped barge which has been used as ITTC validation model. The most important aim of this research is to find out about the time-to-flood of damaged vessels. Therefore floodwater dynamics and water ingress through various openings and opening shapes in the ship superstructure are accounted.

Starting point of this research is a thorough review of the available literature striking models and methods, which assess damage stability and survivability of passenger ships, aiming to identify strength and weaknesses of existing theories. Based on this knowledge it is decided to utilise Computational Fluid Dynamics (CFD) which gives to date more information and details of the physics of progressive flooding than any other numerical method. A commercial numerical CFD code is used to create a set-up with appropriate boundary conditions.

In this approach, it is attempted to account for all possible physical effects with state-of-the art numerical methods. Depending on the geometry of the model, compressible air is used in the simulation, where trapped air is expected or, where the influence of trapped air could be crucial. Moreover, a  $k-\epsilon$  turbulence model is adopted in areas of high flow velocities in order to model the water and air flow through the damage opening and internal openings as true-to-life as possible. Additionally, a six degrees-of-freedom solver has been integrated which simulates ship motions by grid remeshing and grid smoothing methods.

The numerical model described in this paper represents the most advanced treatment to date of modelling the process of progressive flooding with the use of CFD. It can be concluded that the applied method agrees perfectly with all validation cases and that accuracy is satisfactory though simulations with simplified models are carried out. Inferential, the prediction of time-to-flood is mainly derived in a period where the ship remains in quasi-hydrostatic conditions.

<sup>1</sup> Research Assistant, NAME, Universities of Glasgow and Strathclyde

<sup>2</sup> Professor, NAME, Universities of Glasgow and Strathclyde

### 1. INTRODUCTION

Damage stability of passenger ships or Ro-Ro ferries is still a topic of great research interest to the maritime industry and scientific community. The trend in naval industry is to

build bigger and faster ships and superlatives are more important than ever to attract and carry more people. In case of an accident it is not so easy to control and evacuate thousands of people – some of which in panic - during a probably short time in which the ship remains



viable for evacuation and abandonment. Hence, attention has to be turned to safety; onboard but especially to the design phase of a ship where important precautions can be arranged to prevent or limit dangerous situations.

It was the goal to provide a tool which makes it possible to improve the design of a ship regarding its stability in a damage case while accounting for any influential physical factors involved in a flooding scenario by using different methods and approaches adopted from various scientific areas.

## 2. NUMERICAL MODEL

### 2.1 Background

The numerical model of the flooding and internal airflow is based on Reynolds Averaged Navier Stokes Equations (RANSE). In the following paragraphs only basics of the method are briefly described.

The flooding process is initiated by a transient flooding phase and followed up by the progressive phase which dominates the process. For that reason it can be assumed that ship motions are generally small. This is an ideal precondition to introduce dynamic mesh methods in order to simulate ship motions in six degrees-of-freedom.

When a compartment is flooded and air cannot escape it will be compressed as a result of incoming water until the pressure in the air pocket is equal to the effective total pressure on the other side of the opening. This can have significant effects on the flooding process. Such trapped air can delay the flooding process sustainably. Therefore air has to be treated as a compressible ideal gas.

Normally flood water enters the damaged ship at high velocities which results in violent flows with high Reynolds Numbers. After the

transient flooding phase changes to the progressive phase the flood water flow settles down and the Reynolds Number decreases. Nevertheless it has to be accounted for high Reynolds Numbers by using an appropriate turbulence model.

### 2.2 Governing Equations

The flooding process can be described by four governing equations: the conservation of mass (continuity equation), the conservation of momentum, the internal energy equation, and the equation of state [5].

The continuity equation in general form is:

$$\frac{\partial \rho}{\partial t} + \text{div}(\rho u) = S_m \quad (1)$$

where  $\rho$  is density,  $u$  is velocity and  $S_m$  is the mass added to the continuous phase from the dispersed second phase (e.g., due to vaporization of liquid droplets) and any user-defined sources.

The momentum equation can be expressed as:

$$\frac{\partial}{\partial t}(\rho \vec{v}) + \nabla \cdot (\rho \vec{v} \vec{v}) = -\nabla p + \nabla \cdot (\bar{\bar{\tau}}) + \rho \vec{g} + \vec{F} \quad (2)$$

where  $p$  is the static pressure,  $\bar{\bar{\tau}}$  is the stress tensor, and  $\rho \vec{g}$  and  $\vec{F}$  are the gravitational body force and external body forces like centrifugal and Coriolis forces, electromagnetic forces, etc.  $\vec{F}$  also contains other model-dependent source terms such as porous-media and user-defined sources.

The energy equation evolved from the first law of thermodynamics and denotes the increase in energy of a fluid particle is equal to the net rate of heat added to the fluid particle, plus the net rate of work done on the fluid particle. Following equation expresses

the rate of increase of energy of a fluid particle per unit volume:

$$\frac{\partial(\rho i)}{\partial t} + \text{div}(\rho i u) = -p \text{div} u + \text{div}(k \text{grad } T) + \Phi + S_i \quad (3)$$

The combination of previous three equations gives the Navier Stokes equations [1]:

$$\rho \frac{Du}{Dt} = -\frac{\partial p}{\partial x} + \text{div}(\mu \text{grad } u) + S_{Mx} \quad (4)$$

$$\rho \frac{Dv}{Dt} = -\frac{\partial p}{\partial y} + \text{div}(\mu \text{grad } v) + S_{My} \quad (5)$$

$$\rho \frac{Dw}{Dt} = -\frac{\partial p}{\partial z} + \text{div}(\mu \text{grad } w) + S_{Mz} \quad (6)$$

For an ideal gas like air the equation of state can be written as:

$$p = \rho RT \text{ and } i = C_v T \quad (7)$$

where  $p$  is the static pressure,  $T$  is the temperature and  $R$  is the ideal gas constant,  $i$  is the internal energy and  $C_v$  is the specific heat at a constant volume.

Turbulent flows are calculated by the two-equation Standard  $k$ - $\varepsilon$  Turbulence Model. The turbulence kinetic energy  $k$  and its rate of dissipation  $\varepsilon$  are obtained from the transport equations shown below:

$$\frac{\partial}{\partial t}(\rho k) + \frac{\partial}{\partial x_i}(\rho k u_i) = \frac{\partial}{\partial x_i} \left[ \left( \mu + \frac{\mu_t}{\sigma_k} \right) \frac{\partial k}{\partial x_i} \right] + G_k + G_b - \rho \varepsilon - Y_M + S_k \quad (8)$$

and

$$\frac{\partial}{\partial t}(\rho \varepsilon) + \frac{\partial}{\partial x_i}(\rho \varepsilon u_i) = \frac{\partial}{\partial x_i} \left[ \left( \mu + \frac{\mu_t}{\sigma_\varepsilon} \right) \frac{\partial \varepsilon}{\partial x_i} \right] + C_{1\varepsilon} \frac{\varepsilon}{k} (G_k + C_{3\varepsilon} G_b) - C_{2\varepsilon} \rho + S_\varepsilon \quad (9)$$

where  $\sigma_k$  and  $\sigma_\varepsilon$  are the turbulent Prandtl numbers for  $k$  and  $\varepsilon$ , respectively  $G_k$  represents the generation of turbulence kinetic energy due to the mean velocity gradients.  $G_b$  is the generation of turbulence kinetic energy

due to buoyancy.  $\gamma_M$  represents the contribution of the fluctuating dilatation in compressible turbulence to the overall dissipation rate.  $C_{1\varepsilon}$ ,  $C_{2\varepsilon}$ , and  $C_{3\varepsilon}$  are constants and  $S_k$  and  $S_\varepsilon$  are user-defined source terms.

Ship motion in six degrees-of-freedom is simulated by dynamic mesh methods. Each couple of time steps the mesh is transformed or interpolated by using following methods:

- Laplacian Smoothing Method
- Spring Based Method
- Local Remeshing Method

The ship motion itself respectively the translational and angular motion of the centre of gravity of a cell is computed by taking its forces and moments into account. For translational motion the equation is defined as:

$$\dot{\vec{v}}_G = \frac{1}{m} \sum \vec{f}_G \quad (10)$$

where  $\dot{\vec{v}}_G$  is the translational motion of the centre of gravity,  $m$  is the mass, and  $\vec{f}_G$  is the force vector due to gravity.

For angular motion  $\dot{\vec{\omega}}_B$  the equation can be described as:

$$\dot{\vec{\omega}}_B = L^{-1} \left( \sum \overline{M}_B - \overline{\omega}_B \times L \overline{\omega}_B \right) \quad (11)$$

where  $L$  is the inertia tensor,  $\overline{M}_B$  is the moment vector of the body, and  $\overline{\omega}_B$  is the rigid body angular velocity vector.

### 3. MODEL TESTS

Model tests were carried out in the facilities of Helsinki University of Technology (HUT) Ship Laboratory in January 2006. The experiments were meant for the validation of a numerical simulation tool. A detailed description of the model tests and the numerical tool is presented by Ruponen [3; 4].



The model is a box-shaped barge (Figure 1) which consists of three blocks; the forward and aft block constructed of wood and the mid-section made from acrylic plastic in order to make it see-through. The acrylic plastic block contains eight compartments that are connected via internal openings. Details of the flooded compartments and openings are shown in Figure 2. The main dimensions can be found in Table 1.

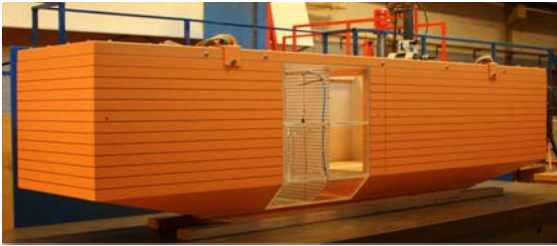


Figure 1: Box-shaped barge with backbone structure

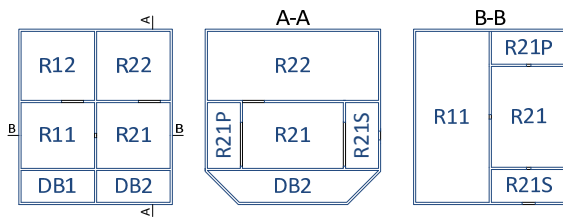


Figure 2: Identification of compartments

Length over all ( $L_{OA}$ )	4.000	m
Breadth	0.800	m
Height	0.800	m
Design draft	0.500	m
Block coefficient at design draft	0.906	
Volume of buoyancy	1.450	m <sup>3</sup>

Table 1: Dimensions of the model

Due to a large initial metacentric height the motions of the models are small and slow which makes it an ideal validation purpose for numerical simulation tools.

Main reason for performing model tests with the box-shaped barge is to validate the

calculation of air compression and airflow. Based on this requirement the compartments are not equipped with large air ventilation ducts. Additionally, water level height is measured in every compartment and motion (heel, trim and draft) of the floating structure is captured.

Rectangular-shaped openings represent fully or partly open doors, manholes and staircase openings, while circular-shaped openings represent broken pipes. All openings are sharp-crested.

## 4. CASE STUDY

### 4.1 Simulation Parameters

The calculations were carried out on an eight node dual core cluster and full computing power has been used.

The geometry of the box-shaped barge has been checked for errors and highly skewed elements followed by an optimisation of the domain order by applying the Reverse Cuthill-McKee method.

Two phases were defined, compressible air with a density following the ideal gas law and a viscosity of  $\nu = 1.7894 \cdot 10^{-5} \text{ kg m}^{-1} \text{ s}^{-1}$  and water with a density of  $\rho = 1.025 \text{ kg/m}^3$  and a viscosity of  $\nu = 1.003 \cdot 10^{-3} \text{ kg m}^{-1} \text{ s}^{-1}$ . The VOF algorithm [2] treating the interface between these two phases was applied. In the beginning of the simulation a highly turbulent flow was expected at the damage opening therefore the standard  $k-\varepsilon$  turbulence model with standard wall functions as near wall treatment was employed. The surrounding air pressure was set equal to atmospheric pressure of 101.325 kPa. The operating density was adjusted to  $\rho_0 = 1.225 \text{ kg/m}^3$  in order to override density which is averaged on all cells.

Pressure inlet boundary conditions were set at the bottom of the water tank providing a constant head pressure of 19.620 kPa to keep the water level in the tank at a constant height. On top of the air domain the boundary conditions were set to pressure outlet conditions to allow air to escape or enter the domain. All other faces were set to wall boundary conditions apart from the internal openings and the damage opening, which were set to interior boundary conditions.

Finally the dynamic mesh algorithm was applied by defining rigid zones that were allowed to be moved and remeshed and rigid zones that were only allowed to be moved. The moving water and moving air mesh that surrounded the ship hull was allowed to be moved and remeshed while the ship hull and the flooded compartments were only allowed to move. For the correct calculation of the six degrees-of-freedom motion the mass and the moment of inertia in three axes had to be defined, see Table 2.

Mass of the box-shaped barge	1450 kg
Moment of inertia along the x-axis $I_{xx}$	176 kg m <sup>2</sup>
Moment of inertia along the y-axis $I_{yy}$	2235.3 kg m <sup>2</sup>
Moment of inertia along the z-axis $I_{zz}$	2209.4 kg m <sup>2</sup>

Table 2: Mass and moment of inertia of the box-shaped barge

Equations are solved implicitly and pressure based.

Solution control	Mode
Discretization	
Pressure	PRESTO!
Density	Second Order Upwind
Momentum	Second Order Upwind
Turbulence Kinetic Energy	Second Order Upwind
Turbulence Dissipation Rate	Second Order Upwind
Energy	Second Order Upwind
Volume Fraction	Geo-Reconstruct
Pressure-Velocity Coupling	Coupled
Courant Number	1.000.000

Table 3: Solution control for flow and volume fraction equations

The initial condition was that the air domain and the moving air domain were completely filled with compressible air and the water tank and moving water domain were completely filled with water. A time step of 0.0025 seconds was chosen according to the requirements of the dimensionless Courant Number and the requirements of the applied remeshing algorithm. When ship motion is large and a relatively large time step is used the remeshing algorithm might not be able to remesh all cells so that holes could appear in the remeshed zones. The solution of the governing equations would then diverge and the calculation would certainly crash. To avoid this, the time step has to be sufficiently small.

## 4.2 Modelled Domain

Ideally, five domains, see Figure 3 are used to model the flooding case: the flooded structure of the ship, the water tank, room for air above the water tank, a moving air and water domain around the ship. These moving domains are rigid and follow the motion of the ship during the dynamic mesh update. The mesh of the water tank and the room for air around the moving domain are deformed according to the data obtained by the six degrees-of-freedom algorithm. The space on the ship which will not be affected by flooding is not modelled and therefore assigned as void space.

When water flows into the ship the water level of the water tank can slightly vary. By introduction of a pressure inlet on the bottom of the water tank and a pressure outlet on top of the air domain above the water tank the water level can be controlled and water and air can enter and exit the domain freely.

The damage openings can be placed on the bottom of the hull for bottom damage and on the side of the hull for side damage and are assigned as interior boundary condition. Optionally, openings for air ventilation, which





are as well assigned as interior boundary condition, can be placed on top of the superstructure of the ship.

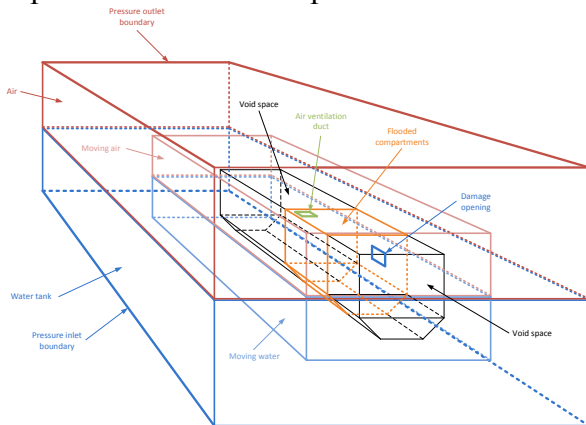


Figure 3: Schematic view of dynamic flooding domain

### 4.3 Side Damage

Ruponen's [3] test case No. 6 is used for validation which is side damage through a large opening in the forward compartment of the barge.

The configuration of the doors of the test case is as follows:

Identification		Connecting	Open
FDP	Fire door port	R21↔R21P	yes
FDS	Fire door starboard	R21↔R21S	yes
DP	Damaged pipe	R11↔R21	yes
SC1	Staircase aft	R11↔R12	yes
SC2	Staircase forward	R21↔R22	yes
DAS	Damage opening starboard	R21S↔Sea	yes
MH	Manhole	DB2↔R21	no

Table 4: Configuration of openings

The centre of the damage opening is located 185 mm below the sea level in intact condition.

Heeling is very small even in the transient phase of flooding because the model is very stable. A comparison between measured and calculated results of ship motions and water level heights in the compartments is shown in Figure 4- Figure 12.

## 5. DISCUSSION OF RESULTS

In the beginning ship motion in transversal direction, see Figure 6, is almost symmetrical because floodwater is allowed to spray directly from the sea through room R21S to room R21 and then further to room R21P. In addition, the internal fire doors FD1 and FD2 are larger in magnitude than the damage opening, so the floodwater tends to spread quicker on the lower deck than it can be replenished through the damage opening. For that reason the roll angle of the box-shaped barge remains small, even in the first 40 seconds during the transient flooding phase, and settles down at a stable level around approximately  $0.05^\circ$  in the progressive flooding phase. At the same time instant the trim angle increases significantly slower than in the beginning of the flooding which can be explored in Figure 4.

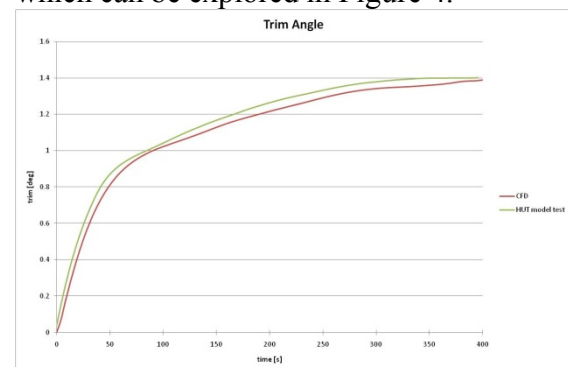


Figure 4: Trim angle of the box-shaped barge

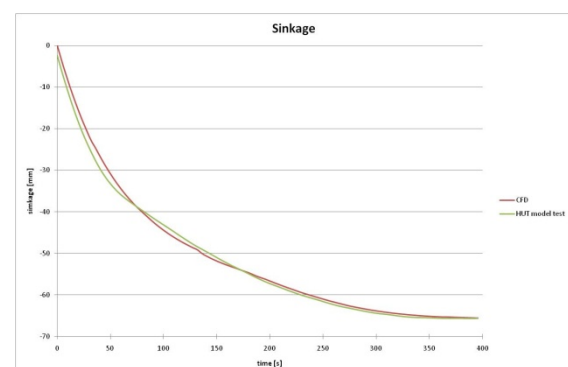


Figure 5: Sinkage of the box-shaped barge

In almost the same manner the sinkage of the barge behaves: the barge sinks quickly at the start of the flooding process, followed up by a slower vertical motion from time instant

40 seconds until the barge attains her final stable position, see Figure 5.

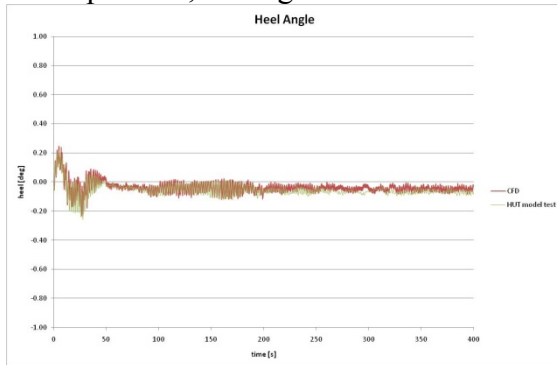


Figure 6: Heel angle of the box-shaped barge

The graphs below show that rooms that were directly affected by the floodwater ingress were filled up much faster than the other rooms which were progressively flooded. In Figure 7 it can be seen that the flooding slows down between a water height of 0.13 m and 0.14 m. When the water reaches the upper edge of the fire doors flooding slows down as well. This can be clearly identified by a bend in the charts at a water height of 0.2 m, see Figure 7 and Figure 9.

Room R21 is filled up constantly represented by an almost straight chart line even though at a certain point water is dispensed to room R11. Room R11 fills quickly by the time when the water in room R21 reaches SC2 and water can flow into room R22. Then the filling process in room R11 slows down until the room is completely full with floodwater.

Room R12 and R22 are slowly flooded as the height difference of the water level inside the compartment and outside of the hull is gradually decreasing. The flooding process stops when the water level inside the compartment is equal to the water level outside of the hull.

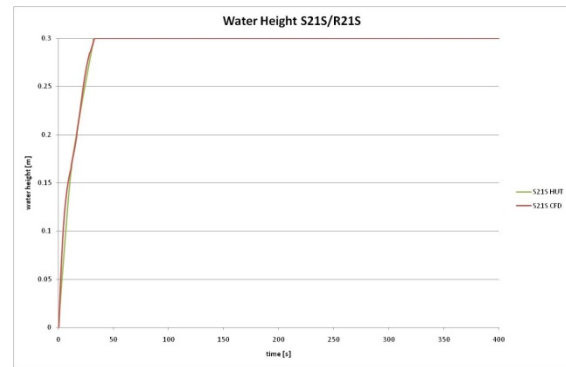


Figure 7: Water height in room R21S

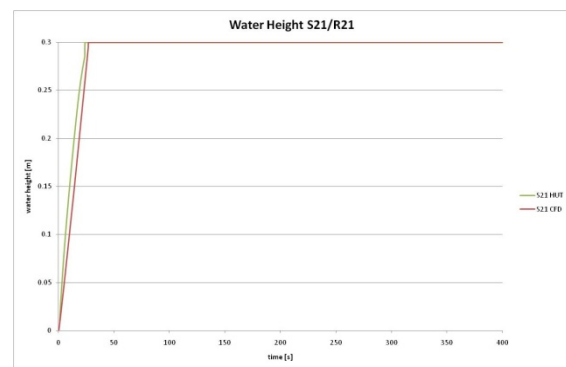


Figure 8 Water height in room R21

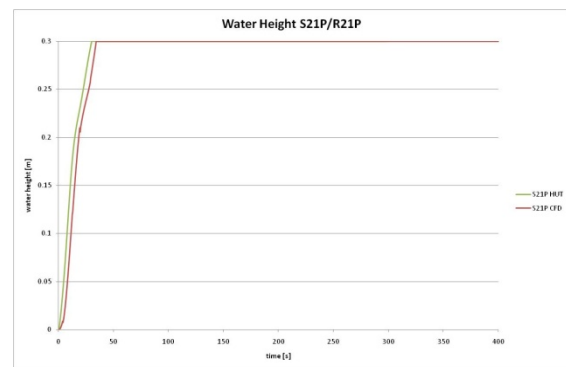


Figure 9 Water height in room R21P

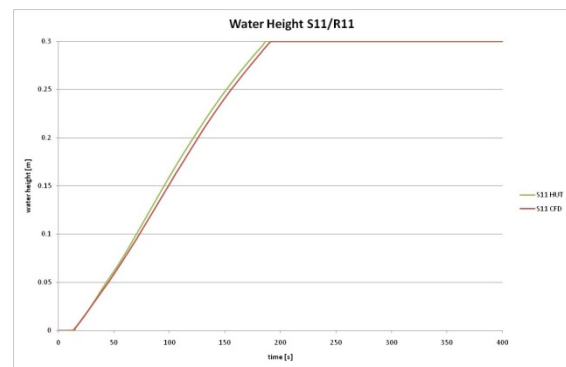


Figure 10 Water height in room R11

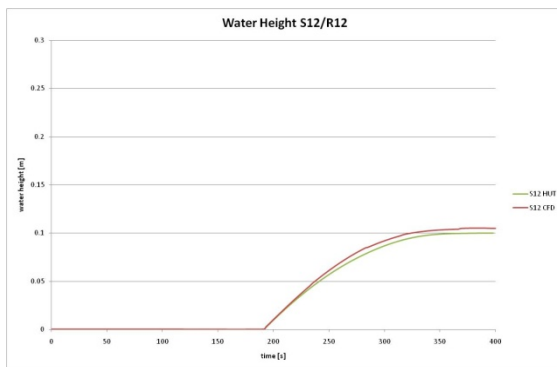


Figure 11 Water height in room R12

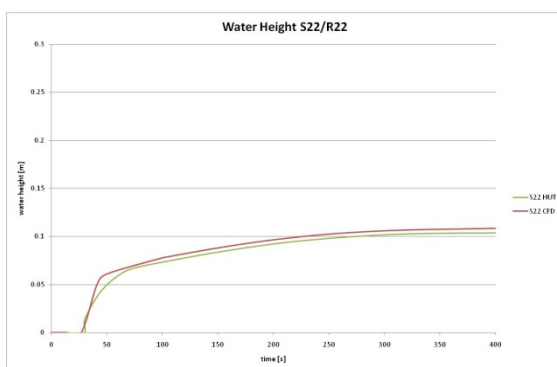


Figure 12 Water height in room R22

The measured water height is a good indicator for the accuracy of the calculations. The correspondence of the calculated with the measured results is very good. It could be noticed that flooding always slowed down when the damage opening was fully submerged. Also, when the floodwater reached the upper edge of an internal opening the flooding process decelerated significantly.

## 6. CONCLUSION

A variety of different modelling techniques and methods have been applied to accomplish the intention of creating a true-to-detail flooding simulation with a state-of-the-art CFD tool. Attention has also been paid to the applicability and universality which makes the method adaptive in a broad field.

Following issues have been achieved:

- ✓ A flooding model in dynamic conditions (freely moving non-propelled model) has

been designed that allows simulating both the highly dynamic phase during transient flooding and the almost quasi-static phase during progressive flooding.

- ✓ All physical phenomena such as free-surface effects, compressible air, turbulent flows and ship motions in six degrees-of-freedom have been taken into consideration.
- ✓ It has been proved that the dynamic mesh method is capable of dealing with large ship motions and that it can be combined with numerical techniques such as the volume of fluid method and the adoption of compressible fluids.
- ✓ The developed numerical method proved to be effective when applied to the damage case of a box-shaped barge that was also used as a validation model for ITTC.

## 7. ACKNOWLEDGEMENTS

The authors wish to acknowledge Dr. Pekka Rupponen from NAPA Ltd. who provided valuable validation data for the case studies.

## 8. REFERENCES

- [1] Fluent, 2006, "*Fluent 6.3 User's Guide*", Fluent Inc., Lebanon.
- [2] Hirt, C.W., and Nichols, B.D., 1981, "*Volume of fluid (VOF) method for the dynamics of free boundaries*", *Journal of Computational Physics*, Vol.39, 1: 1981. pp. 201-225.
- [3] Ruponen, P., 2006, "*Model Tests for the Progressive Flooding of a Box-Shaped Barge*", Report No. M-292, Helsinki University of Technology, Helsinki, Finland, p. 88.
- [4] Ruponen, P., Sundell, T., and Larmela, M., 2007, "*Validation of a Simulation Method for Progressive Flooding*", *International Shipbuilding Progress*, Vol.54: 2007. pp. 305-321.
- [5] Versteeg, H.K., and Malalasekera, W., 2007, "*An introduction to computational fluid dynamics : the finite volume method*", Pearson Education Ltd., Harlow, England ; New York.